Discovery and optimization of inhibitors of the Parkinson's disease associated protein DJ-1

Shinya Tashiro,[a,b] Jose M. M. Caaveiro,[a,b,c*] Makoto Nakakido,[a,b] Aki Tanabe,[a] Satoru Nagatoishi,[a,b] Yasushi Tamura,[d] Noriyuki Matsuda,[e] Dali Liu,[f] Quyen Q. Hoang,[h,g] and Kouhei Tsumoto[a,b,i,*]

[a]*Department of Bioengineering, Graduate School of Engineering, The University of Tokyo, Tokyo 113-8656, Japan,* [b]*Institute of Medical Science, The University of Tokyo, Tokyo 108-8639, Japan.* [c]*Laboratory of Global Healthcare, Graduate School of Pharmaceutical Sciences, Kyushu University, Fukuoka 812-8582, Japan.* [d]*Department of Material and Biological Chemistry, Faculty of Science, Yamagata University, Yamagata 990-8560, Japan,* [e]*Ubiquitin Project, Tokyo Metropolitan Institute of Medical Science, 2-1-6 Kamikitazawa, Setagaya, Tokyo 156-8506, Japan,* [f]*Department of Chemistry and Biochemistry, Loyola University Chicago, Chicago IL 60660,* [g]*Department of Biochemistry and Molecular Biology, and* [h]*Stark Neurosciences Research Institute, Indiana University School of Medicine, Indianapolis, IN 46202,* [i]*Department of Chemistry & Biotechnology, School of Engineering, The University of Tokyo, Tokyo 108-8639, Japan.*

*Corresponding authors: jose@phar.kyushu-u.ac.jp (JMMC), and tsumoto@bioeng.t.u-tokyo.ac.jp (KT)

Current address for ST: *Department of Material and Biological Chemistry, Faculty of Science, Yamagata University, Yamagata 990-8560, Japan*

This is the author's manuscript of the article published in final edited form as:

Tashiro, S., Caaveiro, J. M. M., Nakakido, M., Tanabe, A., Nagatoishi, S., Tamura, Y., … Tsumoto, K. (2018). Discovery and optimization of inhibitors of the Parkinson's disease associated protein DJ-1. ACS Chemical Biology. https://doi.org/10.1021/acschembio.8b00701

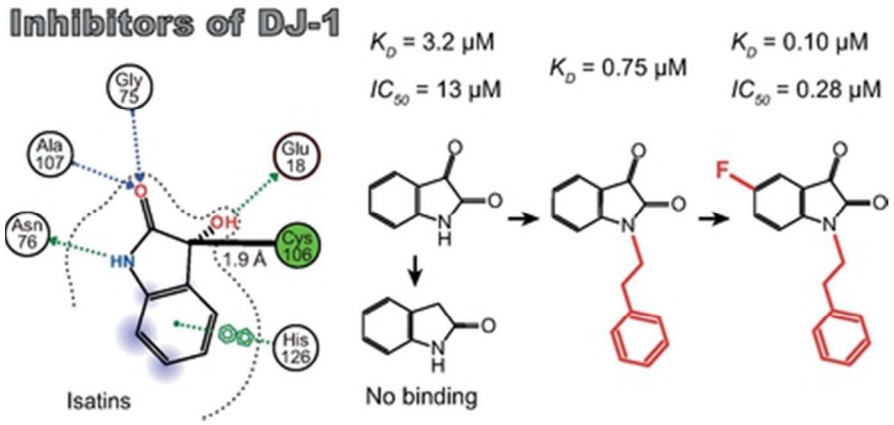

Graphical Abstract

37x17mm (300 x 300 DPI)

ABSTRACT

DJ-1 is a Parkinson's disease associated protein endowed with enzymatic, redox sensing, regulatory, chaperoning, and neuroprotective activities. Although DJ-1 has been vigorously studied for the last decade and a half, its exact role in the progression of the disease remains uncertain. In addition, little is known about the spatiotemporal regulation of DJ-1, or the biochemical basis explaining its numerous biological functions. Progress has been hampered by the lack of inhibitors with precisely known mechanisms of action. Herein we have employed biophysical methodologies and X-ray crystallography to identify and to optimize a family of compounds inactivating the critical Cys106 residue of human DJ-1. We demonstrate these compounds are potent inhibitors of various activities of DJ-1 in vitro and in cell-based assays. This study reports a new family of DJ-1 inhibitors with a defined mechanism of action, and contributes towards the understanding of the biological function of DJ-1.

INTRODUCTION

Parkinson's disease is a devastating neurodegenerative disorder of ever-increasing concern in modern societies[1]. The substantia nigra and striatum of brains of patients suffering from advanced stages of the disease are severely damaged, showing low levels of the neurotransmitter molecule dopamine. Although a very active field of research, the molecular mechanisms triggering Parkinson's disease are still largely unknown because of the inherent complexity of the disorder. The elucidation of the underlying etiology and the establishment of effective therapies to combat Parkinson's disease and Parkinsonism are pressing challenges faced by the medical and scientific community, and an problem of great concern for the society at large.

The protein DJ-1 was initially identified as the product of an oncogene, and soon after it was revealed that mutations on this protein lead to early onset Parkinson's disease.[2,3] For example pathological mutations M26I, D149A and L166A cause abnormal conformation of the protein resulting in a functional loss.[4] DJ-1 also protects dopaminergic neurons from the toxicity of rotenone (a small molecule inducing symptoms of Parkinsonism).[5-7] A number of structural, biochemical and cellular studies have sought to understand the protective effect of DJ-1 in dopaminergic neurons.[8-13]

A common theme in these and other studies is the central role played by the conserved residue Cys106 of DJ-1,[4,14,15] showing that changes in the oxidation state and/or mutations of Cys106

modulate the neuroprotective effects of DJ-1. The residue Cys106 is found in several oxidation states that includes the reduced thiol from, the activated and reversible sulfenic and sulfinic forms, and the irreversible sulfonic form.[4] Interfering with this delicate equilibrium affects the performance of the protein in a cell-environment. Intriguingly, numerous cellular functions have been proposed for DJ-1 (see Supporting information Table 1 for an extended list). Despite an explosion in the number of studies about DJ-1, the debate about its actual biological function has not been resolved to date. In particular, the regulatory mechanism of DJ-1, or how its loss of function causes dopaminergic neuronal death and Parkinsonism, are key questions not clarified yet. Previous studies have also reported overexpression of DJ-1 in many types of cancers compared with normal tissue. The overexpression of DJ-1 is critical for anti-cancer drug resistance.[16-20] This observation has been corroborated by knockdown of DJ-1 using siRNA, improving the sensitivity of cancer cells to certain drugs.[16,18,19,21,22] These previous studies suggested that the inhibition of protective function of DJ-1 could be a promising therapeutic approach to fight cancer.

One of the reasons hampering the definitive characterization of DJ-1 could be the absence of a potent and well-characterized chemical inhibitor. Small-molecule inhibitors and molecular probes are useful tools to analyze functions of proteins,[23] such as the classical examples of compounds FK506,[24] wortmannin,[25] and JQ1.[26] These inhibitors provided important clues to elucidate the

functions and pathways of target proteins *in vitro* and at the cellular level. The current body of research suggests that an inhibitor and/or a molecular probe binding to the pocket of Cys106 will inhibit the biological function of DJ-1.[27-29] Although several compounds have been reported to interfere with the biological functions of DJ-1, the precise mechanism of action of these compounds at the molecular level has not been clarified.[4,30,31]

Herein we have employed fragment-based methodologies to identify compounds with a well-defined inhibition mechanism against DJ-1. We focused on compounds capable of binding at the pocket of the putative active residue Cys106, since virtually all proposed functions of DJ-1 are connected to this residue. We identified and validated a compound from a primary screen displaying an affinity in the μM range. By employing rational design methodologies, the affinity and inhibitory potency of second-generation compounds was improved by more than 30-fold. These compounds showed robust inhibitory properties in vitro and suggested inhibition of the proposed deglycase detoxifying activity of DJ-1 in cell-based assays. These inhibitors may contribute to elucidate the biological function of DJ-1 and its role in Parkinsonism.

RESULTS AND DISCUSSION

Identification of a novel compound binding to DJ-1

The structure of DJ-1[9-12] suggested the existence of a pocket around the critical Cys106 residue

with favorable properties for binding small molecules.[32] We carried out a screening of a fragment library containing several hundred compounds (< 300 Da) by surface plasmon resonance (SPR) with the gola of finding a hit compound of medium-low affinity (Supporting information Figure 1). After the screening stage, compound **1** emerged as a suitable hit (Figure 1). The dissociation constant (K_D) determined by SPR was 2.0 ± 0.5 μM (Figure 1b, Supporting information Figure 2). Individual association (k_{on}) and dissociation (k_{off}) rates could not be determined at this stage because the kinetic phases were fast (box-shape sensorgrams). Isothermal titration calorimetry (ITC) was employed as an orthogonal method. The value of K_D obtained by calorimetry was 3.2 ± 0.1 μM, consistent with that determined by SPR. The thermodynamic parameters obtained by ITC indicated that the interaction between **1** and DJ-1 is highly exothermic (ΔH = −11.6 ± 0.1 kcal mol^{-1}) and opposed by the entropy change ($-T\Delta S$ = 4.1 kcal mol^{-1}) (Figure 1c, Supporting information Figure 3). The binding of **1** also increased the thermal stability of DJ-1 with respect to the unbound protein (ΔT_M = 1.8 °C) as determined by differential scanning fluorimetry (DSF) [33] (Figure 1d). These data demonstrated that **1** binds robustly to DJ-1 with moderate affinity and very high enthalpic efficiency (EE = 1.1 kcal mol^{-1}),[34] although the binding mechanism was still unclear after this stage.

Structural characterization

To identify the binding location of **1** within the structure of DJ-1 we employed X-ray crystallography. The complex between DJ-1 and **1** was obtained by the soaking method at high (40 mM) and low (2 mM) concentration of ligand, achieving a resolution of 1.39 Å and 1.65 Å, respectively (Figure 2a,b, Supporting information Tables 2-4). The overall structure of DJ-1 in complex with **1** was virtually identical to the unbound form (PDB ID: 4P2G)[28] with RMSD values in the range between 0.103 and 0.093 Å. Compound **1** was tightly held by to DJ-1 by a covalent bond to the sulfur atom of Cys106. The crystal soaked with high concentration of ligand displayed two other molecules of **1** covalently bound to the surface of DJ-1 in the form of a Schiff base to the amine group of residues Lys148 and Lys182 (Supporting Information Figure 4).[35] The mutation of key residues of the binding pocket at Cys106, the use of the analog **2**, and the soaking experiment at low concentration collectively demonstrated that recognition of **1** occurs specifically at Cys106, whereas the secondary binding sites resulted from unspecific binding and were not observed by ITC (Figure 2, Supporting Information Figures 5, 6).

The bond length between C3 of **1** and the sulfur atom of Cys106 was 1.89 ± 0.04 Å, a value approaching that of the sum of the covalent radius of carbon (0.76 Å) and sulfur (1.05 Å) (Figure 2b, c).[36] To validate the formation of the covalent bond between Cys106 and **1** in solution, we employed UV-visible spectroscopy. Because the structure revealed that formation of the covalent bond is accompanied by the partial loss of aromaticity in the indole ring of **1**, we predicted the

UV-visible spectrum would be changed when covalently bound to DJ-1 (Figure 2d). As expected, the intensity of the absorption peak of **1**, centered at ~305 nm, was greatly reduced in the presence of DJ-1. Similarly, the intensity of this absorption peak was also diminished in the presence of the reducing agent dithiothreitol (DTT).

The box-shaped binding profile of **1** to DJ-1 obtained by SPR was consistent with the reversible attachment to Cys106. To demonstrate whether binding of **1** to DJ-1 is also reversible in the crystalline form, crystals of the protein were first soaked overnight with **1**, followed by three successive soaks in the absence of ligand (Supporting information Figure 5). No evidence of **1** was found in the pocket of Cys106, demonstrating that reversibility is also observed in the crystalline form.

Residues Cys106 (covalently bound to **1**), Glu18 (hydrogen bonded to **1**) and His126 (establishing π-π interactions with the aromatic ring of **1**) were individually mutated, and their binding properties examined by ITC (Figure 2e, Supporting information Figure 6, Supporting information Tables 5, 6). Except for the conservative mutation H126Y, the other five mutations completely abrogated binding of **1** to DJ-1, establishing the importance of the interactions between **1** and the residues lining the pocket for the stable recognition of the ligand. The high-resolution crystal structure of the mutein C106S soaked with **1** did not show evidence of ligand bound in the pocket (Supporting information Figure 5), although we note that two

molecules of **1** appeared unspecifically bound to Lys residues as seen above for the wild-type protein.

The evidence gathered so far thus demonstrated that the binding properties of **1** are explained by the fast and reversible reaction with Cys106 of DJ-1 (Figure 2f). This reaction is governed by Glu18, which depresses the pKa of the sulfur atom of Cys106 of DJ-1 enhancing its nucleophilicity,[37] and facilitating its attack to the atom C3 of **1**. The complex is additionally stabilized by non-covalent π-π interactions between the ring of the ligand and His126, and presumably by the very short hydrogen bond with residue Glu18.

Structure-activity relationship

The crystal structure of the complex revealed a small gap between the position C5 of **1** and DJ-1, suitable for a small substituent that could increase the affinity of the compound. We obtained compounds **3-5** and determined their affinity to DJ-1 by ITC as above (Figure 3a,b, Supporting information Figure 3). The dissociation constant of **3** was similar to that of **1**, whereas **4** and **5** displayed a robust increase in affinity (~3-fold) with respect to **1** (K_D of **4** and **5** were 0.93 ± 0.05 μM and 1.00 ± 0.06 μM, respectively). The crystal structure of **4** in complex with DJ-1 was subsequently determined at 1.45 Å resolution (Figure 3c). The overall structure of DJ-1 in complex with **4** was virtually identical to that with **1** bound (RMSD = 0.11 Å). In addition, the

interaction of **4** with the three key residues Glu18, Cys106, and His126 did not change significantly. A covalent bond between Cys106 and **4** was also observed (distance = 1.96 ± 0.05 Å), as well as the short hydrogen bond with Glu18 (2.42 ± 0.05 Å). The fluorine atom attached to **4** interacted with residues Arg28 and Pro184 of the second chain of the DJ-1 dimer. The distances between the fluoride atom of **4** and Arg28 and Pro184 of DJ-1 were 3.05 ± 0.05 Å and 3.51 ± 0.05 Å, respectively. It is generally considered that non-covalent interactions between fluoride and proteins are generally stabilizing, thus explaining the increase of affinity **4**.[38,39]

Next, we obtained compounds **6-8** displaying electrophilic substituents at position C7. An electrophilic substituent at C7 could, in principle, promote the formation of a covalent bond with Cys106.[40] However, no increase (or decrease) of affinity was observed among the three compounds evaluated (Supporting information Figure 3). Crystal structures revealed that each compound accommodates in the pocket in the same manner as that of compound **1** (Supporting information Figure 7). From these experiments we concluded that modifications at this position did not promote higher affinity between DJ-1 and the ligands.

It was also apparent from the crystal structure that there was some space to accommodate a substituent at position N1 (Figure 4). To analyze the effect of a methyl-substituent at position N1, the 1.5 Å resolution crystal structure of the complex between DJ-1 and **9** was determined (Figure 4b-d). The overall structure of DJ-1 remained essentially unchanged with respect to that of DJ-1

with compound **1** (RMSD = 0.09 Å). However, a close inspection revealed that binding of **9** induced local changes in the conformation of the neighboring residue Asn76. In particular, the side-chain of Asn76 is shifted because of the influence of the methyl group of **9**. The distance between the N1 atom of the ligand and the oxygen atom of Asn76 increased from 2.99 ± 0.04 Å in the complex of DJ-1 with **1**, to 4.35 ± 0.05 Å in the complex with **9**. This local but clear conformational change resulted in a ~4-fold lost of affinity of (Supporting information Figure 3).

We hypothesized that the movement of Asn76 could be exploited to enlarge the binding pocket with a homolog of **1** displaying bulkier substituents at N1. A total of 52 compounds with different substitutions at the N1 position were obtained from a compound library at The University of Tokyo, and their effect on the thermal stability of DJ-1 examined by DSF. The criterion to select suitable hits was the stabilization of DJ-1 by more than 1 ˚C when compared with the value determined for **1** (Figure 4a,e). ITC experiments with candidates **10-14** were subsequently performed to precisely determine the binding constants (Figure 4f, Supporting information Figure 3). Compounds **10** and **11** were selected based on their availability, sufficient solubility, and higher affinity for DJ-1.

To understand how **10** and **11** bind to DJ-1, we determined their crystal structure in complex with DJ-1, in both cases at 1.65 Å resolution (Figure 4h, Supporting information Figure 7). The overall structure of DJ-1 in complex with **10** or with **11** remained the same as above, including

the covalent bond between the compounds and Cys106 (2.01 ± 0.08 Å and 1.99 ± 0.07 Å, respectively) and the short hydrogen bond with Glu18 (2.45 ± 0.08 Å and 2.42 ± 0.07 Å, respectively). To accommodate the large aryl aliphatic group of attached to N1 in **10**, the side-chain of residue Asn76 adopted the open conformation, enlarging the binding groove of DJ-1 (Figure 4h). In contrast, the conformation of Asn76 did not significantly change in the complex with the smaller compound **11**. The additional contact interface between **10** and DJ-1 increased the number of van der Waals interactions, which could explain its higher affinity. Compounds **13** and **14,** both displaying long and linear substituents at N1, also bound to DJ-1 more tightly than **1**. On the one hand, the structure of DJ-1 in complex with **13** confirmed the generality of the binding conformation of these family of compounds (Supporting information Figure 7, Supporting information Table 4). On the other hand, the branched substituent at position N1 in **12** hampered binding to DJ-1.

We have described how to increase the affinity of analogs of **1** by adding substituents at positions N1 or C5. The next step was to combine these substitutions in a single compound. Taking the structures of **1**, **4**, **10**, and **11** as blueprints, we designed **15** and **16** (Figure 5). The affinities of both compounds increased substantially to K_D values of ~100 nM, representing an increase of more than 30-fold with respect to **1**. Visual inspection of the SPR profiles of **15** and **16** clearly indicates that their k_{off} is significant slower than that of previous hits, suggesting

higher selectivity of the optimized inhibitors (Supporting information Figure 2). In particular, a value of 0.06 s^{-1} was determined for **15**. The crystal structure of **15** bound to DJ-1 was determined at 1.60 Å, showing no significant difference to the overall structure of other complexes of DJ-1 with isatin compounds. The special features of **15** are such that it combines the favorable interactions of **1**, **4**, and **10** all in one compound, explaining the highest affinity among the compounds examined (Figure 5b).

Inhibitory potency

Because the compounds bind strongly to the critical Cys106, it was expected they would exert a strong inhibitory effect on the function of DJ-1. Among the proposed functions of DJ-1, this protein (enzyme) has shown robust glyoxalase activity amenable to classical enzymatic analysis.[41-43] Glyoxal is the byproduct of the metabolism of glucose produced in the cells,[44] its excess causing oxidative stress by nonspecific modification of proteins, lipids, and DNA, resulting in the inactivation of these important biomolecules. Glyoxalase activity with the compound phenylglyoxal as a substrate[45] was employed to monitor the inhibitory potency of several compounds (Figure 5c). The values of IC_{50} determined for **1**, **15**, and **16** were 13, 0.28, and 0.33 μM, respectively, consistent with the order of affinities determined by ITC (Figure 5a). No inhibitory effect was observed with analog **2** in agreement with binding experiments (Figure

2e).

More recently, a protective function of DJ-1 in guanine glycation has also been reported.[46] No inhibitors have been examined for this novel function of DJ-1 to date. The HPLC profile of dGTP (containing a guanine moiety) was compared under various experimental conditions in the presence of the major glycating agent methylglyoxal (MGO), with or without DJ-1 and with or without compound **1** (Supporting information Figure 8). In the presence of DJ-1, full protection is achieved. However, the similarity of the HPLC profile of the mixture dGTP/MGO in the absence of DJ-1 with that in the presence of DJ-1 and **1** clearly indicated that the protecting activity of DJ-1 is abolished in the presence of the inhibitor. Overall, these experiments demonstrate that these compounds are effective inhibitors of the enzymatic activity and protective function of DJ-1 in vitro.

Efficacy in cells

We aimed at evaluating the effect of these compounds in cell-assays. First we demonstrated target engagement in a cellular environment by the technique of cellular thermal shift assay (CETSA).[47,48] A preliminary temperature scan in the absence of inhibitors was carried out, proving the feasibility of the assay and establishing an optimal temperature of 63 °C for the subsequent experiments with compounds (Supporting information Figure 9). The incubation of

HeLa cells with compounds followed by thermal treatment at 63 °C showed a concentration-dependent stabilization of the soluble from of the protein in all three compounds tested (Supporting information Figure 10). The greatest stabilization efficacy was achieved with **15**, followed by that of **16** and **1**.

Lysine residues of proteins are converted to carboxy-methyl-lysine (CML) in the presence of glyoxal.[41,43,45] Since DJ-1 has been proposed to prevent glycation of proteins caused by glyoxal, we studied the level of CML in the presence of inhibitors of DJ-1 in HEK293 cells by western blot (Figure 5d, Supporting information Figure 11). In the absence of glyoxal, no protein bands of proteins modified with CML were detected, regardless of the presence or absence of compounds. The bands corresponding to DJ-1 and β-actin remained constant under all conditions tested. In contrast, in the presence of glyoxal (2 mM), several bands corresponding to proteins modified with CML were clearly visible. In the presence of compounds **1**, **16** or **16** the intensity of these bands increased significantly compared with the control experiment (DMSO). This effect suggested that the compounds were permeable in the cells, where they inhibited the preventive activity of DJ-1 toward glycation of proteins. We note that the relative intensity of the band corresponding to DJ-1 (and β-actin) in the SDS-PAGE gel was constant.

The activity of DJ-1 was independently verified using a HeLa cell line (Supporting information Figure 12). Similarly to the results above, the intensity of a protein modified with CML clearly

increases at the highest concentration of **1** and **15** employed. In contrast, such effect was not observed in DJ-1 knockout cells treated with inhibitors. Interestingly, the level of CML modification in the knockout cells was lower than that in wild type cells suggesting that an alternative route of cellular repair is stimulated in the absence of DJ-1. Indeed, a similar compensatory mechanism has been recently described in dicarbonyl detoxification mediated by glyoxalase-1 in mammalian Schwann cells.[49]

In summary, we have identified and optimized the first family of inhibitors of the Parkinson's disease associated protein DJ-1 using structure-based rational approaches. The maximal affinity and inhibitory potency (IC_{50}) achieved were 100 and 300 nM, respectively. Crystal structures of the protein/inhibitor complex, site-directed mutagenesis, and spectrometric measurements revealed that these compounds bound to a conspicuous pocket of DJ-1, where they attached covalently to residue Cys106 (Figures 2-4). Since Cys106 is the critical residue for virtually all the functions proposed for DJ-1, it was expected that the inactivation of this residue would lead to impairment of the function of the protein. Indeed these compounds inhibited the glyoxalase and guanine protective activities of DJ-1 *in vitro*, stabilized the protein against thermal aggregation in a cell environment, and decreased in the deglycase detoxifying activity in cell-based assays (Figure 5). Because the small size of the most potent inhibitor (270 Da) it is reasonable to aim for better affinity, selectivity, and physicochemical properties by applying

additional optimization schemes, and especially by exploiting larger substituents at position N1.

It is important to note that the family of inhibitors described herein belong to the family of isatin, a endogenous metabolite.[35] Since the concentration of isatin (**1**) increases in the urine of patients of Parkinson's disease,[50] it was suggested **1** could be employed as a marker of the disease.[51,52] Our study has demonstrated that the dissociation constant of **1** is close to its concentration in mammalian serum,[51,53,54] suggesting that, in principle, the biological activity of DJ-1 could be modulated by endogenous levels of **1**, and supporting the notion of **1** being a marker for Parkinson's disease. Moreover, **1** is also a known inhibitor of monoamine oxygenase B, the enzyme degrading the brain neurotransmitter dopamine and several of its precursors yielding highly reactive oxidative species such as H_2O_2 and various aldehydes. Because the inhibitory potency of **1** for monoamine oxygenase B is similar to that in DJ-1,[55-59] we suggest the possibility of a simultaneous regulation of both enzymes by a common metabolite overproduced during the progression of the disease. Previous studies have also showed that the addition of a phenyl group to position N1 improved the anticancer activity of isatin derivatives.[60-63] Our structural analysis might help to study the mechanism why the addition to N1 improved the anticancer activity of isatin derivatives.

In conclusion, we reported a new family of inhibitors of the human protein DJ-1 with a defined mechanism of action, and suggested a route to design even more potent inhibitors of the isatin

family.

MATERIALS AND METHODS

Expression and purification of DJ-1

Human DJ-1 and muteins were cloned in a modified pET28b vector containing an N-terminal His_6-tag and a TEV cleavage site between the N-terminal tag and the sequence of the protein.[28] Briefly, *Escherichia coli* BL21 (DE3) transformed with plasmid containing DJ-1 was grown in LB medium at 37 °C. Protein expression was induced with isopropyl β-D-thiogalactopyranoside (1 mM) when OD_{600} reached a value of 0.6. Cells were grown for additional 16 hr at 28 °C, after which they were harvested by centrifugation and stored at −80 °C. Frozen cells were thawed on ice and resuspended in a buffer composed of 20 mM TRIS-HCl at pH 7.9 (buffer was prepared at 4 °C, unless otherwise indicated), 500 mM NaCl, 5 mM imidazole, and 1 mM dithiothreitol (DTT). Cells were homogenized with an ultrasonic cell-disruptor instrument (Tommy, Japan). The soluble fraction was separated by centrifugation and loaded into a nickel affinity chromatography (His-Trap HP, GE Healthcare). Protein was eluted with a gradient of 5-500 mM imidazole over 10 column volumes.

Two different routes were employed depending on the absence or presence of a His_6-tag in the purified protein. For the preparation of DJ-1 without His_6-tag, fractions containing DJ-1 were

pooled and subjected to a digestion with TEV protease in a buffer containing 20 mM TRIS-HCl at pH 7.9, 150 mM NaCl, and 1 mM DTT for 12 hours. The digestion product was loaded in a nickel affinity chromatography, achieving the separation of the cleaved His_6-tag. Fractions containing DJ-1 were further purified in a size exclusion chromatography column (Hiload 16/600 superdex 200 pg, GE Healthcare) equilibrated with a buffer containing 20 mM TRIS-HCl at pH 7.9, 150 mM NaCl, and 3 mM DTT. Purified DJ-1 protein was supplemented with 5 mM DTT and stored at −80 °C. For the preparation of DJ-1 with His_6-tag on the N-terminus, fractions containing DJ-1 from a nickel affinity chromatography were further purified in a size exclusion chromatography column (Hiload 16/600 superdex 200 pg, GE Healthcare) equilibrated with a buffer containing 20 mM TRIS-HCl at pH 7.9, 150 mM NaCl, and 3 mM DTT. Purified DJ-1 protein was supplemented with 5 mM DTT and stored at −80 °C.

Fragment screening by SPR

Fragment screening was conducted with a Biacore T200 instrument (GE Healthcare, Piscataway, NJ) using a CM5 sensor chip as previously described.[64] The Zenobia fragment library (Zenobia Therapeutics) containing 352 compounds was employed for the screening. The fragments were diluted at 200 μM in screening buffer (25 mM HEPES pH 7.5, 150 mM NaCl, 0.005% Tween-20, 1 mM DTT and 5% DMSO). DJ-1 was immobilized to a surface decorated with an anti-His_6 antibody.[65,66] The BSA-free anti-His_5-tag antibody (QIAGEN, 40724 Hilden) was covalently

immobilized on a CM5 sensor chip by the amine coupling method at a density of ~12,000 RU. DJ-1 displaying a His_6-tag was captured by the antibody at about 1,500 RU. Subsequently, DJ-1 was covalently immobilized to the antibody by the amine coupling method. All the immobilization was conducted in a buffer composed of 25 mM HEPES pH 7.5, 150 mM NaCl, and 0.005% Tween-20 (immobilization buffer).

Sensorgrams corresponding to the binding of compounds to DJ-1 were obtained by injecting the analyte (compounds) at a flow rate of 30 μL min^{-1}. Contact and dissociation times were 15 s in both cases. Data analysis was performed with the BIAevaluation software (GE Healthcare). The binding level of each fragment was corrected with standard procedures by employing 4−6% DMSO in eight steps in the Biacore T200 evaluation software.[65]

Binding affinity (*SPR*)

SPR was employed also to determine the dissociation constant between selected compounds and DJ-1 in a Biacore T200 instrument (GE Healthcare). DJ-1 was immobilized as above, except that the protein was not covalently attached to the antibody to avoid oxidative inactivation of Cys106. DJ-1 was washed off after each regeneration cycle, and subsequently immobilized before evaluating each compound. Compounds were flowed in two-fold serial dilutions in PBS buffer PBS (NaCl 137 mM, KCl 2.68 mM, Na_2HPO_4 10.1 mM, and KH_2PO_4, 1.76 mM, pH 7.4 - 7.5) supplemented with Tween 20 at 0.005% (PBS-T) and 5% DMSO. The concentrations tested for

compound **1** were in the range 0.3125 to 20 μM, for compounds **4**, **5**, **10**, and **11** in the range 0.078 to 5 μM, and for compounds **15** and **16** in the range 0.016 to 1 μM. Sensorgrams were obtained by injecting increasing concentrations of analytes at a flow rate of 30 μL min^{-1}. Contact and dissociation time were 60 and 120 sec, respectively. Regeneration was carried after completion of each sensorgram by injecting a solution of 1 M Arg-HCl at pH 4.4.

Data analysis was performed with the BIAevaluation software (GE Healthcare) assuming a Langmuir model. The K_D value for compounds **1**, **4**, **5**, **10**, **11**, and **16** was calculated as the concentration at half the maximum response. For compound **15**, a full kinetic analysis was performed. Association (k_{on}) and dissociation (k_{off}) rate constants were calculated by a global fitting analysis. The value of K_D was determined from the ratio of the rate constants ($K_D = k_{off} / k_{on}$).

Binding affinity (ITC)

Thermodynamic parameters of the interaction between DJ-1 and compounds were determined in an auto-iTC200 (GE Healthcare) at 25 °C. Prior to each experiment, the protein sample was equilibrated in a solution of PBS by dialysis (>100-fold volume) and to remove DTT. Compounds were prepared in the same PBS buffer supplemented with 5% DMSO. The concentration of protein in the cell and that of compounds in the syringe are indicated in the corresponding figure legends. To determine the dissociation constant K_D of compound **1** to

muteins, the measurement was performed with higher concentration of protein (100 μM) and compound (1 mM). Binding isotherms were fitted to a one-site binding model using ORIGIN 7.0.

Crystallization and preparation of complexes

Crystals of DJ-1 in complex with compounds were prepared by soaking method. First, crystals of unbound and reduced DJ-1 were obtained from purified protein in 20 mM potassium phosphate buffer at pH 7.0 and 5 mM DTT using the hanging drop method by mixing protein at 20 mg mL^{-1} with a solution of 100 mM TRIS-HCl at pH 8.5, 200 mM sodium citrate, 30% PEG-400, and 5 mM DTT. Suitable crystals of DJ-1 were soaked with the crystallization solution supplemented with compounds (1 to 40 mM) for 1 to 24 hr. We also performed a back-soaking experiment, in which crystals of DJ-1 were first soaked overnight with **1** (10 mM), followed by three consecutive soaks for approximately one hour in the same buffer but in the absence of compound. Suitable crystals were harvested, frozen, and stored in a vessel containing liquid N_2 until data collection.

Data collection and structure refinement

Data was collected in beamlines BL5A, AR-NE3A and AR-NW12 at the Photon Factory (Tsukuba, Japan) under cryogenic conditions (100 K) at a wavelength of 1.000 Å. Diffraction images of single crystals of each complex were processed with the program MOSFLM and merged and scaled with the program SCALA or AIMLESS[67] of the CCP4 suite. The three

dimensional structure was determined by the method of molecular replacement using the coordinates of DJ-1 (PDB code, 1SOA) with the program PHASER.[68] Initial models were further refined with the program REFMAC5[69] and COOT.[70] Validation was carried out with PROCHECK.[71] In all cases, residue Cys106 (or Ser106 in mutein C106S) appeared in the non-allowed region of the Ramachandran plot despite the very clear features of the electron density at this position and the high resolution achieved (1.30 to 1.65 Å). No other residue appeared in the non-allowed region of the Ramachandran plot. The coordinates and parameters of the ligands were generated with PRODRG.[72] The data collection and refinement statistics are given in Supporting information Tables 2-4.

UV-visible spectroscopy

Purified DJ-1 (100 μM), **1** (2 mM), and (DTT 1 mM) were separately prepared in PBS, mixed appropriately, incubated for 5 minutes, and their UV-visible spectra collected at room temperature in a V-660 Spectrophotometer (Jasco, Japan) between 270 nm and 350 nm.

Thermal stability by DSF

The thermal stability of DJ-1 in the presences or absence of compounds was monitored by DSF with SYPRO Orange (Invitrogen), in a CFX Connect Real-Time System (Bio-Rad).[28] Excitation and emission filters were set to 470 and 570 nm, respectively. Compounds were dissolved in DMSO at 2 mM, and stored at −30 ˚C until use. Protein DJ-1 without His_6-tag at 10 μM and

compounds at 50 μM were mixed in PBS, 0.01% Tween 20, and 2.5% DMSO. During the experiment the temperature was increased from 30 to 85 °C at a constant rate of 2 °C/min. The melting temperature (T_M) was determined from the derivatives (inflection point) of the unfolding curve.

Enzymatic activity of DJ-1

The enzymatic activity of DJ-1 was determined at 250 nm using phenylglyoxal (Tokyo Chemical Industry, Japan) as substrate.[45] All assays were performed in an automated EnSpire instrument (Perkin Elmer, MA). The concentrations of DJ-1 and phenylglyoxal were 0.5 μM and 2 μM, respectively. The concentration of compounds **1**, **2**, **15** and **16** ranged between 1.0 nM and 30 μM. Buffer was composed of 100 mM potassium phosphate buffer at pH 7.0 supplemented with 1% DMSO. The initial velocities were obtained by monitoring the time course of substrate disappearance from the absorbance at 250 nm. Sigmoidal curves were fitted to the rate constants obtained in the presence of compounds to obtain the inhibition constant with OriginPro (OriginLab, Northampton).

Cell assay (HEK293 cells)

HEK293 cells were cultured in Dulbecco's modified Eagle's medium (DMEM) with 10% fetal bovine serum, 100 units/ml of penicillin and 100 μg/ml of streptomycin (Thermo Fisher Scientific, Waltham), in a humidified atmosphere with 5% CO_2 at 37°C. Cells (2×10^5) were

seeded on 6 cm dish and cultured for three days. Before the treatment with glyoxal, the medium was exchanged to DMEM with 1% fetal bovine serum, 100 units/ml of penicillin and 100 μg/ml of streptomycin and the cells were starved. After 20 hours culture in the starvation medium, the medium was exchanged to DMEM with 1% fetal bovine serum, 0.2% DMSO, and compounds at the desired concentrations. After three hours of culture, the cells were harvested for analysis. HEK293 cells were harvested and lysed in assay buffer (10 mM Tris–HCl, pH 7.4, 0.1% sodium deoxycholate, 1% Triton X-100, 0.1% SDS, 150 mM NaCl, and 1 mM EDTA). The lysates were separated by SDS–PAGE and transferred to a nitrocellulose membrane. The membranes were blocked for one hour in 5% skim milk in PBS-T (Tween 20 at 0.05%) at room temperature, followed by incubation at 4 °C for overnight with antibodies against DJ-1 (MBL), β-Actin (Santa Cruz), or carboxy methyl lysine (R&D systems). After washing three times, membranes were incubated with horseradish peroxidase-conjugated secondary antibodies in PBS-T. The proteins were developed and visualized using an Amersham Imager 600 instrument (GE Healthcare, Piscataway, NJ).

Cell assay (HeLa cells)

HeLa cells (1.5×10^5) were seeded on 6 well-plates and cultured in DMEM with 10% fetal bovine serum, 100 units/ml of penicillin, and 100 μg/ml of streptomycin in a humidified atmosphere with 5% CO_2 at 37°C for 24 hours. DJ-1 knockout HeLa cells were obtained as

described previously.[73] Before the treatment with compounds, the medium was exchanged to DMEM with 0.5% fetal bovine serum, 100 units/ml of penicillin and 100 μg/ml of streptomycin. After 20 hours culturing in the starvation medium, the medium was exchanged to DMEM with 0.5% fetal bovine serum and **1** at the desired concentrations. The concentration of DMSO was 0.2%. The cells were harvested three hours later for analysis, lysed in RIPA buffer (Wako, Japan) and the lysates subjected to SDS–PAGE and transferred to a nitrocellulose membrane. The membranes were blocked for one hour in 5% skim milk in PBS-T (Tween 20 at 0.05%) at room temperature, followed by overnight incubation at 4 °C with antibodies against DJ-1 (MBL), β-Actin (Santa Cruz), and carboxy methyl lysine (R&D systems) diluted in PBS-T. After washing three times, the membranes treated with anti-carboxy methyl lysine antibody were incubated with horseradish peroxidase (HRP)-conjugated secondary antibody in PBS-T. Membranes treated with anti-DJ-1 or anti-β-Actin antibodies were incubated with Cy5-conjugated secondary antibody in PBS-T. Chemiluminescence from HRP and fluorescence from Cy5 were detected in a LAS4000 (Fujifilm, Japan) or Typhoon9200 (Amersham) instruments, respectively.

HPLC

The nucleotide dGTP (500 μM) was incubated at 37°C in 50 mM sodium phosphate pH 7.0 for 4 hours, or in the presence of MGO (5 mM), or with MGO (5 mM) and DJ-1 (5 μM), or with MGO (5 mM), DJ-1 (5 μM) and **1** (50 μM). The samples were analyzed by RP-HPLC in a InertSustain

C18 column (GL Science, Japan) equilibrated in 100 mM potassium phosphate, pH 5.5 at 22°C, and eluted with the same buffer.

CETSA

HeLa cells were harvested and suspended with culture media containing 10% FBS to a cell density of 3 x 10^6 cells ml^{-1}. Compounds solubilized in DMSO were added to cells (final DMSO content 0.5 %). Cells were incubated for 30 min at 37˚C in 5% CO_2. The cell suspension was subsequently heated at the indicated temperature for 3 min, followed by cooling down to room temperature for 3 min. After the heating step, cell suspensions were freeze-thawed three times using liquid nitrogen. The resulting cell lysates were centrifuged at 10,000 g for 60 min at 4 °C in order to separate the soluble fraction from cell debris and aggregates. The soluble fraction was subjected to a western blot using a PVDF membrane. The membranes were blocked for one hour in 1% skim milk in TRIS buffered saline supplemented with 0.05 % Tween 20 (TBS-T) at room temperature, followed by overnight incubation at 4 °C with antisera against DJ-1 (MBL), β-Actin (Santa Cruz). After washing three times, membranes were incubated with horseradish peroxidase-conjugated secondary antibodies. The proteins were developed and visualized using ImageQuant LAS 4000 (GE Healthcare, Piscataway, NJ). All CETSA data were expressed as means ± SEM.

ASSOCIATED CONTENT

Supporting Information

The supporting information contains 12 supporting figures and 6 supporting tables. This material is available free of charge via the internet at http://pubs.acs.org.

Accession codes.

Coordinates and structure factors of DJ-1 after back-soaking (accession code 5GPS), DJ-1 in complex with **1** (high concentration, accession code 5GPW), with **1** (low concentration, accession code 5GPV), with **4** (accession code 5GPX), with **6** (accession code 5GPZ), with **7** (accession code 5GQ2), with **8** (accession code 5GQ3), with **9** (accession code 5GQ4), with **10** (accession code 5GQ5), with **11** (accession code 5GQ6), with **13** (accession code 5GQ7), with **15** (accession code 5GQ8), unbound DJ-1 C106S (accession code 5GPT), and DJ-1 C106S in complex with **1** (accession code 5GPU), been deposited in the Protein Data Bank.

Acknowledgements

We thank the staff of the Photon Factory for excellent technical support. Access to beamline BL5A, AR-NW12A, and AR-NE3A was granted by the Photon Factory Advisory Committee (Proposal Numbers 2011G574, 2012G191, 2013G738, 2014G190, and 2016G199). This work was supported by the Platform for Drug Discovery, Informatics and Structural Life Science from

the Ministry of Education, Culture, Sports, Science and Technology of Japan (to K.T.), by JSPS KAKENHI-A grants 25249115 and 16H02420 (to K.T.), by a JSPS KAKENHI-C grant 15K06962 (to J.M.M.C.), and by a Grant-in-Aid for JSPS Fellows (to S.T.).

Author contributions

S.T., J.M.M.C., Q.H.H. and K.T. conceived the study. All authors designed experiments. S.T. performed the primary and secondary screens, SPR, ITC, DSF, enzyme inhibition, and UV-visible experiments. S.T. and J.M.M.C. performed crystallization experiments. J.M.M.C. determined and refined the crystal structures. S.T., A.T. carried out the cell-based assays with assistance from Y.T. and N.M.. S.T. carried out HPLC with the assistance of M.N.. Q.H.H. provided research reagents. All authors analyzed data. S.T. and J.M.M.C. wrote the manuscript. All authors approved the manuscript.

Competing financial interests

The authors declare no competing financial interests.

References

1. Antony, P. M. A., Diederich, N. J., Krueger, R., and Balling, R. (2013) The hallmarks of Parkinson's disease, *FEBS J. 280*, 5981-5993.

2. Nagakubo, D., Taira, T., Kitaura, H., Ikeda, M., Tamai, K., IguchiAriga, S. M. M., and Ariga, H. (1997) DJ-1, a novel oncogene which transforms mouse NIH3T3 cells in cooperation with ras, *Biochem. Biophys. Res. Commun. 231*, 509-513.

3. Bonifati, V., Rizzu, P., van Baren, M. J., Schaap, O., Breedveld, G. J., Krieger, E., Dekker, M. C. J., Squitieri, F., Ibanez, P., Joosse, M., van Dongen, J. W., Vanacore, N., van Swieten, J. C., Brice, A., Meco, G., van Duijn, C. M., Oostra, B. A., and Heutink, P. (2003) Mutations in the DJ-1 gene associated with autosomal recessive early-onset parkinsonism, *Science 299*, 256-259.

4. Hijioka, M., Inden, M., Yanagisawa, D., and Kitamura, Y. (2017) DJ-1/PARK7: A new therapeutic target for neurodegenerative disorders, *NBiol. Pharm. Bull. 40*, 548-552.

5. Gao, H., Yang, W., Qi, Z., Lu, L., Duan, C., Zhao, C., and Yang, H. (2012) DJ-1 protects dopaminergic neurons against rotenone-induced apoptosis by enhancing ERK-dependent mitophagy, *J. Mol. Biol. 423*, 232-248.

6. Kim, R. H., Smith, P. D., Aleyasin, H., Hayley, S., Mount, M. P., Pownall, S., Wakeham, A., You-Ten, A. J., Kalia, S. K., Horne, P., Westaway, D., Lozano, A. M., Anisman, H., Park, D. S., and Mak, T. W. (2005) Hypersensitivity of DJ-1-deficient mice to 1-methyl-4-phenyl-1,2,3,6-tetrahydropyrindine (MPTP) and oxidative stress, *Proc. Natl. Acad. Sci. USA 102*, 5215-5220.

7. Martinat, C., Shendelman, S., Jonason, A., Leete, T., Beal, M. F., Yang, L. C., Floss, T., and Abeliovich, A. (2004) Sensitivity to oxidative stress in DJ-1-deficient dopamine neurons: An ES-derived cell model of primary Parkinsonism, *PLoS Biol. 2*, 1754-1763.

8. Honbou, K., Suzuki, N. N., Horiuchi, M., Niki, T., Taira, T., Ariga, H., and Inagaki, F. (2003) The crystal structure of DJ-1, a protein related to male fertility and Parkinson's disease, *J. Biol. Chem. 278*, 31380-31384.

9. Wilson, M. A., Collins, J. L., Hod, Y., Ringe, D., and Petsko, G. A. (2003) The 1.1-angstrom resolution crystal structure of DJ-1, the protein mutated in autosomal recessive early onset Parkinson's disease, *Proc. Natl. Acad. Sci. USA 100*, 9256-9261.

10. Huai, Q., Sun, Y. J., Wang, H. C., Chin, L. S., Li, L., Robinson, H., and Ke, H. M. (2003) Crystal structure of DJ-1/RS and implication on familial Parkinson's disease, *FEBS Lett. 549*, 171-175.

11. Lee, S. J., Kim, S. J., Kim, I. K., Ko, J., Jeong, C. S., Kim, G. H., Park, C., Kang, S. O., Suh, P. G., Lee, H. S., and Cha, S. S. (2003) Crystal structures of human DJ-1 and *Escherichia coli* Hsp31, which share an evolutionarily conserved domain, *J. Biol. Chem. 278*, 44552-44559.

12. Tao, X., and Tong, L. (2003) Crystal structure of human DJ-1, a protein associated with early onset Parkinson's disease, *J. Biol. Chem. 278*, 31372-31379.

13. Kim, R. H., Peters, M., Jang, Y. J., Shi, W., Pintilie, M., Fletcher, G. C., DeLuca, C., Liepa, J., Zhou, L., Snow, B., Binari, R. C., Manoukian, A. S., Bray, M. R., Liu, F. F., Tsao, M. S., and Mak, T. W. (2005) DJ-1, a novel regulator of the tumor suppressor PTEN, *Cancer Cell 7*, 263-273.

14. Bandyopadhyay, S., and Cookson, M. R. (2004) Evolutionary and functional relationships within the DJ1 superfamily, *BMC Evol. Biol. 4*, 6.

15. Wilson, M. A. (2011) The role of cysteine oxidation in DJ-1 function and dysfunction, *Antioxid. Redox Signal. 15*, 111-122.

16. Chen, Y., Kang, M., Lu, W., Guo, Q., Zhang, B., Xie, Q., and Wu, Y. (2012) DJ-1, a novel biomarker and a selected target gene for overcoming chemoresistance in pancreatic cancer,

J. Cancer Res. Clin. Oncol. 138, 1463-1474.

17. Davidson, B., Hadar, R., Schlossberg, A., Sternlicht, T., Slipicevic, A., Skrede, M., Risberg, B., Florenes, V. A., Kopolovic, J., and Reich, R. (2008) Expression and clinical role of DJ-1, a negative regulator of PTEN, in ovarian carcinoma, *Hum. Pathol. 39*, 87-95.
18. He, X. Y., Zheng, Z., Li, J. F., Ben, Q. W., Liu, J., Zhang, J. N., Ji, J., Yu, B. Q., Chen, X. H., Su, L. P., Zhou, L., Liu, B. Y., and Yuan, Y. Z. (2012) DJ-1 promotes invasion and metastasis of pancreatic cancer cells by activating SRC/ERK/uPA, *Carcinogenesis 33*, 555-562.
19. Hod, Y. (2004) Differential control of apoptogis by DJ-1 in prostate benign and cancer cells, *J. Cell Biochem. 92*, 1221-1233.
20. Zeng, H. Z., Qu, Y. Q., Zhang, W. J., Xiu, B., Deng, A. M., and Liang, A. B. (2011) Proteomic analysis identified DJ-1 as a cisplatin resistant marker in non-small cell lung cancer, *Int. J. Mol. Sci. 12*, 3489-3499.
21. Ismail, I. A., Kang, H. S., Lee, H. J., Kwon, B. M., and Hong, S. H. (2012) 2 '-Benzoyloxycinnamaldehyde-Mediated DJ-1 Upregulation Protects MCF-7 Cells from Mitochondrial Damage, *Biol. Pharm. Bull. 35*, 895-902.
22. Liu, H., Wang, M., Li, M., Wang, D. H., Rao, Q., Wang, Y., Xu, Z. F., and Wang, J. X. (2008) Expression and role of DJ-1 in leukemia, *Biochem. Biophys. Res. Commun. 375*, 477-483.
23. Workman, P., and Collins, I. (2010) Probing the probes: Fitness factors for small molecule tools, *Chem. Biol. 17*, 561-577.
24. Harding, M. W., Galat, A., Uehling, D. E., and Schreiber, S. L. (1989) A receptor for the immunosuppressant FK506 is a cis-trans peptidyl-prolyl isomerase, *Nature 341*, 758-760.
25. Banin, S., Moyal, L., Shieh, S. Y., Taya, Y., Anderson, C. W., Chessa, L., Smorodinsky, N. I., Prives, C., Reiss, Y., Shiloh, Y., and Ziv, Y. (1998) Enhanced phosphorylation of p53 by ATN in response to DNA damage, *Science 281*, 1674-1677.

26. Filippakopoulos, P., Qi, J., Picaud, S., Shen, Y., Smith, W. B., Fedorov, O., Morse, E. M., Keates, T., Hickman, T. T., Felletar, I., Philpott, M., Munro, S., McKeown, M. R., Wang, Y. C., Christie, A. L., West, N., Cameron, M. J., Schwartz, B., Heightman, T. D., La Thangue, N., French, C. A., Wiest, O., Kung, A. L., Knapp, S., and Bradner, J. E. (2010) Selective inhibition of BET bromodomains, *Nature 468*, 1067-1073.

27. Chen, J., Li, L., and Chin, L.-S. (2010) Parkinson disease protein DJ-1 converts from a zymogen to a protease by carboxyl-terminal cleavage, *Hum. Mol. Genet. 19*, 2395-2408.

28. Tashiro, S., Caaveiro, J. M. M., Wu, C.-X., Hoang, Q. Q., and Tsumoto, K. (2014) Thermodynamic and structural characterization of the specific binding of Zn(II) to human protein DJ-1, *Biochemistry 53*, 2218-2220.

29. Bjorkblom, B., Maple, J., Okvist, M., Piston, D., Xu, X. M., Brede, C., Larsen, J. P., and Moller, S. G. (2013) The Parkinson's disease protein DJ-1 binds metals and protects against metal induced cytotoxicity, *J. Biol. Chem. 288*, 22809-22820.

30. Drechsel, J., Mandl, F. A., and Sieber, S. A. (2018) Chemical probe to monitor the parkinsonism-associated protein DJ-1 in live cells, *ACS Chem .Biol.*

31. Kitamura, Y., Watanabe, S., Taguchi, M., Takagi, K., Kawata, T., Takahashi-Niki, K., Yasui, H., Maita, H., Iguchi-Ariga, S. M. M., and Ariga, H. (2011) Neuroprotective effect of a new DJ-1-binding compound against neurodegeneration in Parkinson's disease and stroke model rats, *Mol. Neurodegener. 6*, 1-19.

32. Landon, M. R., Lieberman, R. L., Hoang, Q. Q., Ju, S., Caaveiro, J. M. M., Orwig, S. D., Kozakov, D., Brenke, R., Chuang, G.-Y., Beglov, D., Vajda, S., Petsko, G. A., and Ringe, D. (2009) Detection of ligand binding hot spots on protein surfaces via fragment-based methods: application to DJ-1 and glucocerebrosidase, *J. Comput. Aided Mol. Des. 23*, 491-500.

33. Kranz, J. K., and Schalk-Hihi, C. (2011) Protein thermal shifts to identify low molecular

weight fragments, *Methods Enzymol. 493*, 277-298.

34. Ladbury, J. E., Klebe, G., and Freire, E. (2010) Adding calorimetric data to decision making in lead discovery: a hot tip, *Nat. Rev. Drug Discov. 9*, 23-27.

35. Sumpter, W. C. (1944) The chemistry of isatin, *Chem. Rev. 34*, 393-434.

36. Cordero, B., Gomez, V., Platero-Prats, A. E., Reves, M., Echeverria, J., Cremades, E., Barragan, F., and Alvarez, S. (2008) Covalent radii revisited, *Dalton Trans.*, 2832-2838.

37. Witt, A. C., Lakshminarasimhan, M., Remington, B. C., Hasim, S., Pozharski, E., and Wilson, M. A. (2008) Cysteine pKa depression by a protonated glutamic acid in human DJ-1, *Biochemistry 47*, 7430-7440.

38. Mueller, K., Faeh, C., and Diederich, F. (2007) Fluorine in pharmaceuticals: Looking beyond intuition, *Science 317*, 1881-1886.

39. Bissantz, C., Kuhn, B., and Stahl, M. (2010) A medicinal chemist's guide to molecular interactions, *J. Med. Chem. 53*, 5061-5084.

40. Webber, S. E., Tikhe, J., Worland, S. T., Fuhrman, S. A., Hendrickson, T. F., Matthews, D. A., Love, R. A., Patick, A. K., Meador, J. W., Ferre, R. A., Brown, E. L., DeLisle, D. M., Ford, C. E., and Binford, S. L. (1996) Design, synthesis, and evaluation of nonpeptidic inhibitors of human rhinovirus 3C protease, *J. Med. Chem. 39*, 5072-5082.

41. Richarme, G., Mihoub, M., Dairou, J., Bui, L. C., Leger, T., and Lamouri, A. (2015) Parkinsonism-associated protein DJ-1/Park7 Is a major protein deglycase that repairs methylglyoxal- and glyoxal-glycated cysteine, arginine, and lysine residues, *J. Biol. Chem. 290*, 1885-1897.

42. Subedi, K. P., Choi, D., Kim, I., Min, B., and Park, C. (2011) Hsp31 of Escherichia coli K-12 is glyoxalase III, *Mol. Microbiol. 81*, 926-936.

43. Lee, J.-y., Song, J., Kwon, K., Jang, S., Kim, C., Baek, K., Kim, J., and Park, C. (2012) Human DJ-1 and its homologs are novel glyoxalases, *Hum. Mol. Genet. 21*, 3215-3225.

44. Blackinton, J., Lakshminarasimhan, M., Thomas, K. J., Ahmad, R., Greggio, E., Raza, A. S., Cookson, M. R., and Wilson, M. A. (2009) Formation of a stabilized cysteine sulfinic acid Is critical for the mitochondrial function of the parkinsonism protein DJ-1, *J. Biol. Chem. 284*, 6476-6485.

45. Choi, D., Kim, J., Ha, S., Kwon, K., Kim, E.-H., Lee, H.-Y., Ryu, K.-S., and Park, C. (2014) Stereospecific mechanism of DJ-1 glyoxalases inferred from their hemithioacetal-containing crystal structures, *FEBS J. 281*, 5447-5462.

46. Richarme, G., Liu, C. L., Mihoub, M., Abdallah, J., Leger, T., Joly, N., Liebart, J. C., Jurkunas, U. V., Nadal, M., Bouloc, P., Dairou, J., and Lamouri, A. (2017) Guanine glycation repair by DJ-1/Park7 and its bacterial homologs, *Science 357*, 208-211.

47. Jafari, R., Almqvist, H., Axelsson, H., Ignatushchenko, M., Lundback, T., Nordlund, P., and Molina, D. M. (2014) The cellular thermal shift assay for evaluating drug target interactions in cells, *Nat. Protoc. 9*, 2100-2122.

48. Molina, D. M., Jafari, R., Ignatushchenko, M., Seki, T., Larsson, E. A., Dan, C., Sreekumar, L., Cao, Y. H., and Nordlund, P. (2013) Monitoring drug target engagement in cells and tissues using the cellular thermal shift assay, *Science 341*, 84-87.

49. Morgenstern, J., Fleming, T., Schumacher, D., Eckstein, V., Freichel, M., Herzig, S., and Nawroth, P. (2016) Loss of glyoxalase 1 induces compensatory mechanism to achieve dicarbonyl detoxification in mammalian Schwann cells, *J. Biol. Chem.*

50. Hamaue, N. (2000) Pharmacological role of isatin, an endogenous MAO inhibitor, *Yakugaku Zasshi 120*, 352-362.

51. Sommer, T., Bjerregaard-Andersen, K., Simensen, S. M., Jensen, J. K., Jochimsen, B., Riss, P. J., Etzerodt, M., and Morth, J. P. (2015) Enzymatic detection and quantification assay of isatin, a putative stress biomarker in blood, *ACS Chem. Neurosci. 6*, 1353-1360.

52. Bjerregaard-Andersen, K., Sommer, T., Jensen, J. K., Jochimsen, B., Etzerodt, M., and Morth,

J. P. (2014) A proton wire and water channel revealed in the crystal structure of isatin hydrolase, *J. Biol. Chem. 289*, 21351-21359.

53. Medvedev, A., Igosheva, N., Crumeyrolle-Arias, M., and Glover, V. (2005) Isatin: Role in stress and anxiety, *Stress 8*, 175-183.

54. Watkins, P., Clow, A., Glover, V., Halket, J., Przyborowska, A., and Sandler, M. (1990) Isatin, regional distribution in rat brain and tissues, *Neurochem. Int. 17*, 321-323.

55. Binda, C., Li, M., Hubalek, F., Restelli, N., Edmondson, D. E., and Mattevi, A. (2003) Insights into the mode of inhibition of human mitochondrial monoamine oxidase B from high-resolution crystal structures, *Proc. Natl. Acad. Sci. USA 100*, 9750-9755.

56. Bonaiuto, E., Milelli, A., Cozza, G., Tumiatti, V., Marchetti, C., Agostinelli, E., Fimognari, C., Hrelia, P., Minarini, A., and Di Paolo, M. L. (2013) Novel polyamine analogues: From substrates towards potential inhibitors of monoamine oxidases, *Eur. J. Med. Chem. 70*, 88-101.

57. Glover, V., Halket, J. M., Watkins, P. J., Clow, A., Goodwin, B. L., and Sandler, M. (1988) Isatin - Identity with the Purified Endogenous Monoamine-Oxidase Inhibitor Tribulin, *J. Neurochem. 51*, 656-659.

58. Tipton, K. F., Boyce, S., O'Sullivan, J., Davey, G. P., and Healy, J. (2004) Monoamine oxidases: Certainties and uncertainties, *Curr. Med. Chem. 11*, 1965-1982.

59. Youdim, M. B. H., Edmondson, D., and Tipton, K. F. (2006) The therapeutic potential of monoamine oxidase inhibitors, *Nat. Rev. Neurosci. 7*, 295-309.

60. Matesic, L., Locke, J. M., Bremner, J. B., Pyne, S. G., Skropeta, D., Ranson, M., and Vine, K. L. (2008) N-Phenethyl and N-naphthylmethyl isatins and analogues as in vitro cytotoxic agents, *Bioorg. Med. Chem. 16*, 3118-3124.

61. Sabet, R., Mohammadpour, M., Sadeghi, A., and Fassihi, A. (2010) QSAR study of isatin analogues as in vitro anti-cancer agents, *Eur. J. Med. Chem. 45*, 1113-1118.

62. Vine, K. L., Locke, J. M., Ranson, M., Pyne, S. G., and Bremner, J. B. (2007) An investigation into the cytotoxicity and mode of action of some novel N-alkyl-substituted isatins, *J. Med. Chem. 50*, 5109-5117.

63. Vine, K. L., Matesic, L., Locke, J. M., Ranson, M., and Skropeta, D. (2009) Cytotoxic and anticancer activities of isatin and its derivatives: A comprehensive review from 2000-2008, *Anticancer Agents Med. Chem. 9*, 397-414.

64. Nakano, K., Chigira, T., Miyafusa, T., Nagatoishi, S., Caaveiro, J. M. M., and Tsumoto, K. (2015) Discovery and characterization of natural tropolones as inhibitors of the antibacterial target CapF from *Staphylococcus aureus*, *Sci. Rep. 5*, 15337.

65. Kobe, A., Caaveiro, J. M. M., Tashiro, S., Kajihara, D., Kikkawa, M., Mitani, T., and Tsumoto, K. (2013) Incorporation of rapid thermodynamic data in fragment-based drug discovery, *J. Med. Chem. 56*, 2155-2159.

66. Sakamoto, S., Caaveiro, J. M. M., Sano, E., Tanaka, Y., Kudou, M., and Tsumoto, K. (2009) Contributions of interfacial residues of human interleukin15 to the specificity and affinity for its private alpha-receptor, *J. Mol. Biol. 389*, 880-894.

67. Evans, P. (2006) Scaling and assessment of data quality, *Acta Crystallogr. D Struct. Biol. 62*, 72-82.

68. McCoy, A. J., Grosse-Kunstleve, R. W., Adams, P. D., Winn, M. D., Storoni, L. C., and Read, R. J. (2007) Phaser crystallographic software, *J. Appl. Crystallogr. 40*, 658-674.

69. Murshudov, G. N., Vagin, A. A., and Dodson, E. J. (1997) Refinement of macromolecular structures by the maximum-likelihood method, *Acta Crystallogr. D Struct. Biol. 53*, 240-255.

70. Emsley, P., Lohkamp, B., Scott, W. G., and Cowtan, K. (2010) Features and development of Coot, *Acta Crystallogr. D Struct. Biol. 66*, 486-501.

71. Laskowski, R. A., Macarthur, M. W., Moss, D. S., and Thornton, J. M. (1993) PROCHECK -

A program to check the stereochemical quality of protein structures, *J. Appl. Crystallogr. 26*, 283-291.

72. Schuttelkopf, A. W., and van Aalten, D. M. F. (2004) PRODRG: a tool for high-throughput crystallography of protein-ligand complexes, *Acta Crystallogr. D Struct. Biol. 60*, 1355-1363.

73. Kojima, W., Kujuro, Y., Okatsu, K., Bruno, Q., Koyano, F., Kimura, M., Yamano, K., Tanaka, K., and Matsuda, N. (2016) Unexpected mitochondrial matrix localization of Parkinson's disease-related DJ-1 mutants but not wild-type DJ-1, *Genes to Cells 21*, 772-788.

FIGURES

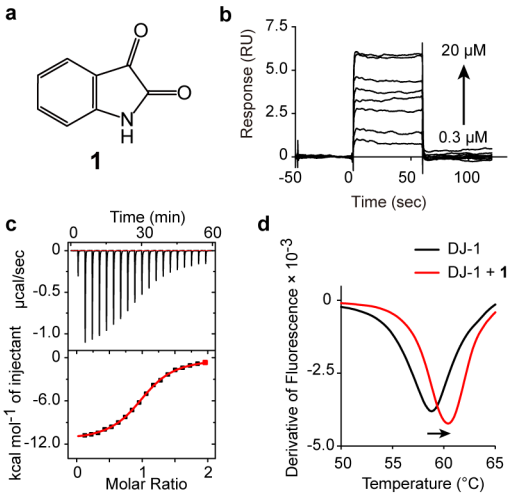

Figure 1 | A novel hit compound binds to DJ-1. (a) Chemical structure of **1** (1*H*-indole-2,3-dione, trivial name *isatin*). **(b)** Binding of **1** to DJ-1 determined by SPR. **(c)** Binding of **1** to DJ-1 determined by ITC. Cell and syringe contained DJ-1 (50 µM) and **1** (500 µM), respectively. Buffer was PBS (NaCl 137 mM, KCl 2.68 mM, Na_2HPO_4 10.1 mM, and KH_2PO_4, 1.76 mM, pH 7.4 - 7.5) supplemented with 5% DMSO. **(d)** Thermal stabilization of DJ-1 (10 µM) in the presence of **1** (50 µM). Buffer was PBS supplemented with 2.5% DMSO.

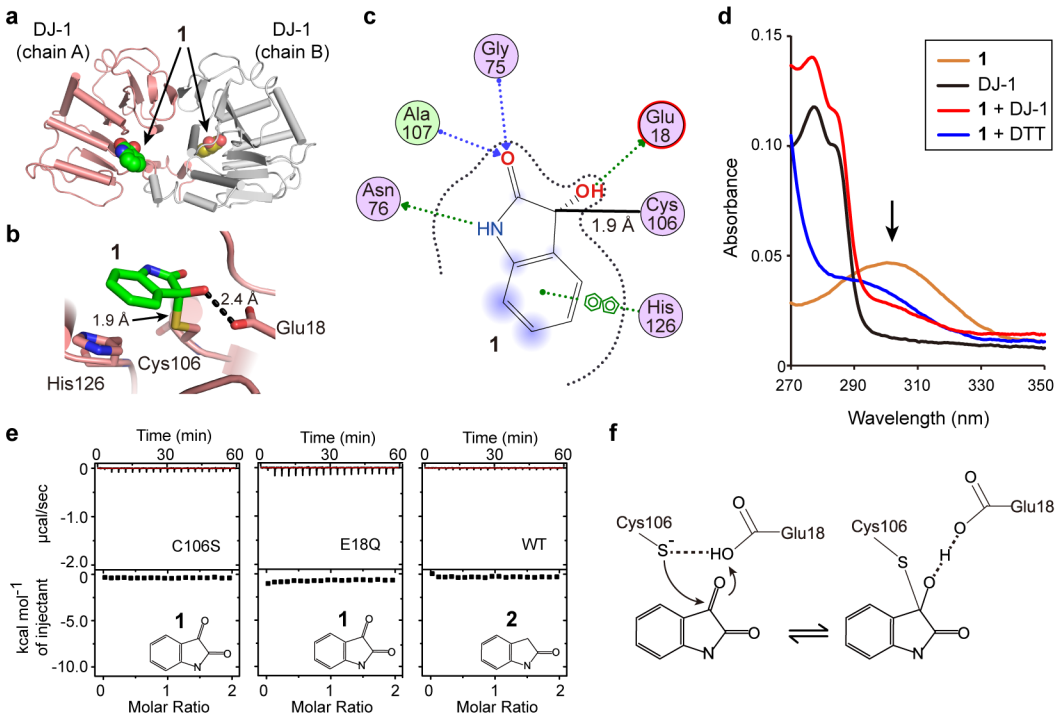

Figure 2 | Structural features of the binding of 1 to DJ-1. (a) Overall structure of the complex between the dimer of DJ-1 (salmon or gray) and **1** (green or yellow space filling representation) at 1.39 Å resolution. **(b)** Close-up view of **1** (green sticks) in the Cys106 pocket. **(c)** Diagram of the covalent bond (thick solid line) and non-covalent forces (dotted arrows) between **1** and DJ-1. **(d)** Change of UV-visible spectrum of **1** after the lost of planarity in the indole ring. The arrow points at the absorption peak of **1**. The orange, black, red, and blue spectra corresponds to **1** (10 µM), DJ-1 (20 µM), **1** (10 µM) mixed with DJ-1 (20 µM), and **1** (10 µM) mixed with DTT (20 mM), respectively. **(e)** Titration of muteins of DJ-1 (100 µM) with **1** (1 mM) (left and center panel), or WT DJ-1 (50 µM) with **2** (500 µM). **(f)** Proposed mechanism for the formation of the covalent bond between **1** and Cys106 of DJ-1. The Glu18 located next to Cys106 enhances the nucleophilicity of the sulfur atom,[37] facilitating the formation of the covalent adduct observed in the high-resolution crystal structure.

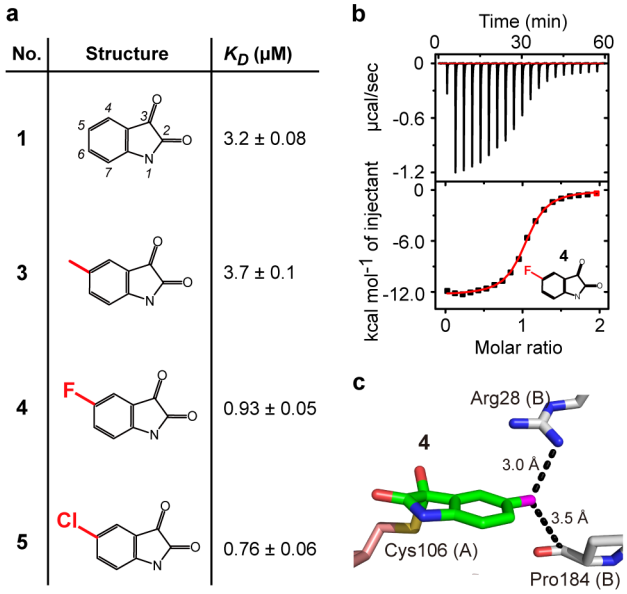

Figure 3 | Binding of 5-substituted compounds to DJ-1. (a) Summary of the dissociation constants. The values of K_D were determined by titration of DJ-1 (50 μM) with compounds (500 μM) in PBS supplemented with 5% DMSO. **(b)** Representative binding isotherm obtained with **4**. **(c)** Close-up view of the binding pocket. The dotted lines correspond to electrostatic interactions between the fluorine atom of **4** and residues Arg28 and Pro184 of chain B of the homodimer of DJ-1, presumably stabilizing the complex.

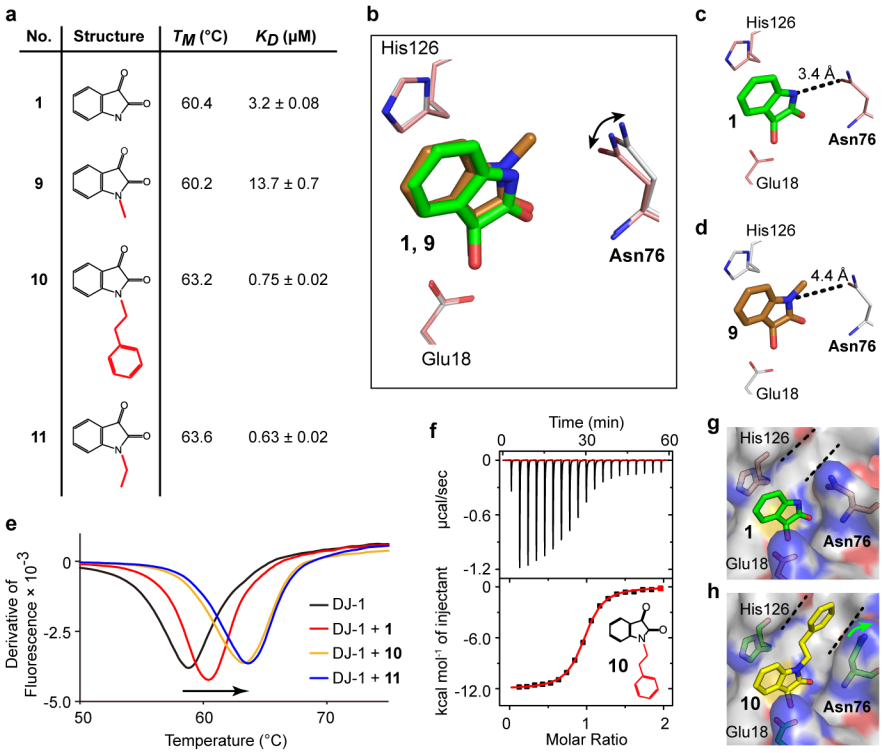

Figure 4 | Binding of 1-substituted compounds to DJ-1. (a) Summary of melting temperatures and dissociation constants for 1-substituted compounds. The value of T_M of DJ-1 at 10 μM as determined by DSF in the absence or in the presence of compounds (50 μM) in PBS supplemented with 2% DMSO. In the absence of compounds, the T_M of DJ-1 was 58.6 ˚C. The K_D values were obtained as in Figure 3. **(b)** Superposition of the crystal structures of DJ-1 in complex with **1** (green) and with **9** (brown). The arrow highlights the adjustment of Asn76 in response to the binding of **9**. For clarity purposes, Cys106 is not shown. **(c-d)** View of the same region depicted in panel for each complex (b). **(e)** Melting curves of DJ-1 in presence of the indicated compounds. **(f)** Representative binding isotherm of **10** to DJ-1. **(g-h)** Comparison of the structures of complex of DJ-1 with **1** and **10**. The orientation of side chain of Asn76 changes in response to binding of **10**, generating a grove that accommodates the large phenyl group.

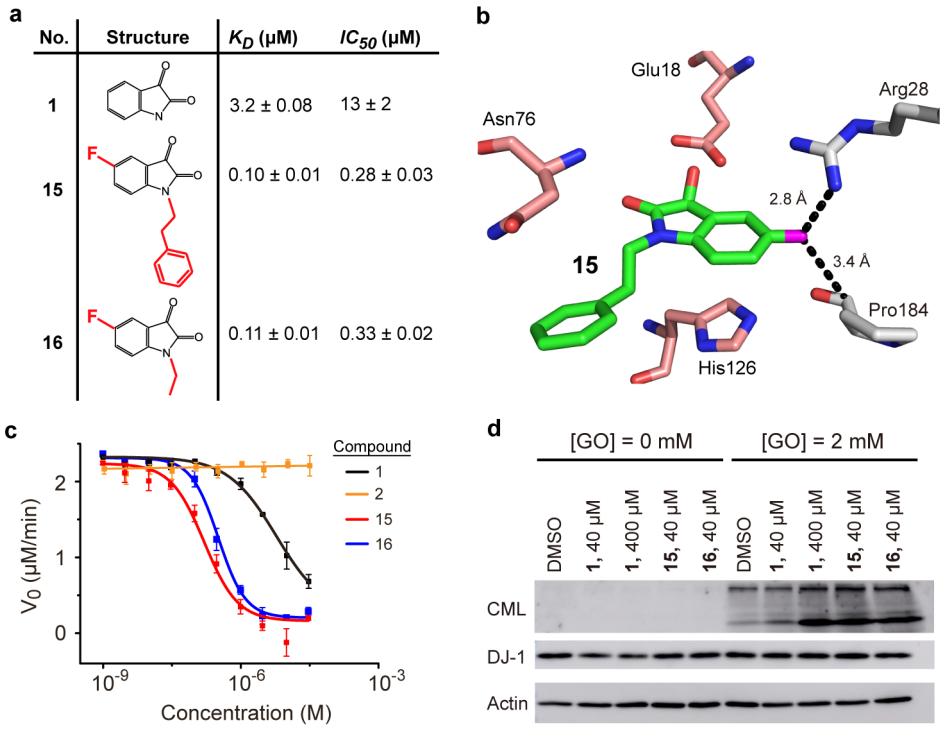

Figure 5 | Characterization of the first generation of potent inhibitors of DJ-1. (a) Binding and inhibitory properties of the compounds indicated. The value of K_D was determined by titration of DJ-1 (20 μM) with compounds (200 μM) in PBS supplemented with 5% DMSO. The values of IC_{50} were calculated from an *in vitro* glyoxalase activity assay (panel c). **(b)** Crystal structure of the complex between DJ-1 and **15**. For clarity purposes, Cys106 is not shown. **(c)** Glyoxalase inhibition assay. Glyoxalase activity of DJ-1 was calculated as the ratio between the initial velocity of disappearance of phenylglyoxal in the presence of inhibitor and the velocity in the absence of inhibitor. **(d)** Glyoxalase/deglycase activity of DJ-1 in HEK293 cells was examined by the appearance of proteins modified with CML (full-sized membranes are shown in Supporting information Figure 11). When DJ-1 is inhibited, the band corresponding to proteins modified with CML increases.